

A Class of Fractional-Order Variational Image Inpainting Models

Y. Zhang, Y.-F. Pu, J.-R. Hu and J.-L. Zhou

College of Computer Science, Sichuan University, Chengdu 610065, China

Received: Jul 18, 2011; Revised Oct. 4, 2011; Accepted Nov. 26, 2011

Published online: 1 May 2012

Abstract: In this paper, we introduce fractional calculus into image inpainting and propose a new class of fractional-order variational image inpainting models, in both space and wavelet domains, inspired by the works of Bai and Feng. The corresponding Euler-Lagrange equations are given and proper numerical algorithm is analyzed. According to the simulations on several testing images, our algorithm demonstrates better inpainting performance on some image details than original integral-order inpainting based on classic calculus.

Keywords: Image inpainting, fractional calculus, total variation, wavelet

1. Introduction

Inpainting which is as ancient as art itself, is a technique of applying undetectable modifications on images. For example, removing the cracks and timestamp from old photos. Bertalmio et al. firstly introduced the image inpainting technique into the image processing[1]. Their main idea is to propagate the surrounding laplacian information along the isophotes into the inpainting domain. Chan and Shen[2] obtained two new inpainting schemes based on the celebrated total variation (TV) minimization model [3] and the segmentation model of Mumford and Shah (MS) [4]. After these well-known works, many image inpainting methods based on partial differential equations (PDEs) have been developed. For example, Chan and Shen took the curvature information into the mathematical model to solve the problem of connectivity [5]. Bertalmio et al. decomposed the image into two parts [6]. The structure part is inpainted by the method of literature[1], and the texture part is restored by texture synthesis technique [7]. Masnou proposed a disocclusion method based on the continuation of the level lines broken by the spots[8]. Bertalmio reformulated the inpainting problem as a particular case of image interpolation in which they intend to propagate level lines [9]. Expressing this in terms of local neighborhoods and using a Taylor expansion, he derived a third-order PDE that performed inpainting. Chan et al. handled the wavelet coefficients loss of images with TV model[20].

Recently, fractional-order PDEs have been studied in computer vision. Cuesta proposed fractional-order linear integro-differential equations which interpolated heat equations and wave equations using the Riemann-Liouville (R-L) fractional derivative [10], while in literatures[11][12], fractional-order scale spaces (α scale space) and the fractional high-order linear filtering were introduced. Mathieu et al. used fractional derivative to detect the image edges [13]. Pu et al. designed the fractional derivative based filter to detect the texture details of images[14]. Zhang et al. introduced fractional-order image inpainting into metal artifacts reduction in CT images[17][18]. Bai and Feng derived the fractional-order anisotropic diffusion model[16], and they found that when the order was 1.8 or 2.2, the performance was the best. Guidotti and Lambers proposed two fractional-order anisotropic diffusion equations with orders between 0 and 1[15]. The fractional derivative can be treated as the generalization of the integer-order derivative. It has been studied by many mathematicians (For example, Euler, Hardy, Littlewood, and Liouville)[19]. There are several definitions which obtained the fractional derivative only using the integer-order derivative including: Riemann-Liouville fractional derivative, Grünwald-Letnikov (G-L) fractional derivative and Caputo fractional derivative.

In this paper, we propose an image inpainting method combined the TV model with fractional derivative called fractional-order TV image inpainting model. The classical TV based inpainting scheme has a drawback while in-

* Corresponding author: e-mail: maybe198376@gmail.com

painting the texture parts of the images: the texture will be smoothed out just as another high frequency noise. The new equation can be treated as a regularization of TV based inpainting scheme. We compared our method with the classical TV inpainting method. According to the simulation results, we got better visual effects and Peak Signal to Noise Ratio(PSNR).

In next section, we will give the details of our model. In Section 3, we will show some simulation results. And the conclusion will be in Section 4.

2. Fractional-order variational image inpainting models

2.1. Review of TV inpainting model and TV wavelet inpainting model

Assume a standard image model as

$$u(x) = u_0(x) + n(x) \quad (1)$$

where u_0 is the origin image, n is additive noise and u is the contaminated image with noise. Let Ω the inpainting (open) domain with its boundary $\partial\Omega$, and E an extended domain surrounding the $\partial\Omega$, so that $\partial\Omega$ lies in the interior of $E \cup \Omega$. The image inpainting model based on total variation proposed by Chan and Shen[2] is as following:

$$\min J_\lambda[u] = \int_{E \cup \Omega} |\nabla u| dx dy + \frac{\lambda_\Omega}{2} \int_E |u - u_0|^2 dx dy \quad (2)$$

The first term is the regularizing term, to inpaint damaged domains while the second term in the energy is a data fidelity term that can keep important features and sharp edges when noise exists. λ_Ω is scale function tuning the weight of two terms. According to the variational theory, the Euler-Lagrange equation corresponding to (2) is

$$-\nabla \cdot (|\nabla u|^{-1} \nabla u) + \lambda_\Omega (u - u_0) = 0 \quad (3)$$

with the Neumann boundary condition $\partial u / \partial n = 0$ on $\partial\Omega$, where $\lambda_\Omega = \lambda \cdot \mathbf{1}_E(x, y) = \begin{cases} \lambda, & (x, y) \in E \\ 0, & \text{otherwise} \end{cases}$. This model is inspired by the classic total variation denoising model[3].

We assume that the size of the images is $n \times m$. Let us denote the standard orthogonal wavelet transform of $u_0(x)$ by

$$u_0(\alpha, x) = \sum_{j,k} \alpha_{j,k} \psi_{j,k}(x), j \in \mathbf{Z}, k \in \mathbf{Z}^2. \quad (4)$$

Packet loss during transmission in compressed form causes loss of wave coefficients of $u_0(x)$ on the index region I , i.e., $\{\alpha_{j,k}\}$'s with $(j, k) \in I$ represent those wavelet components missing or damaged. The task is to restore the lost coefficients.

Total variation wavelet models proposed by Chan *et al.*[20] are followed.

For noisy images, we have

$$\min_{\beta_{j,k}} F(u, z) = \int_{\mathbf{R}^2} |\nabla_x u(\beta, x)| dx + \sum_{(j,k)} \lambda_{j,k} (\beta_{j,k} - \alpha_{j,k})^2, \quad (5)$$

where $u(\beta, x)$ has the wavelet transform:

$$u(\beta, x) = \sum_{j,k} \beta_{j,k} \psi_{j,k}(x), \quad \beta = (\beta_{j,k}), j \in \mathbf{Z}, k \in \mathbf{Z}^2,$$

and the parameter $\lambda_{j,k}$ is zero if $(j, k) \in I$, the missing index set; otherwise, it equals a positive constant λ to be properly selected. I is the inpainting index region. The Euler-Lagrange equation corresponding to (5) is

$$-\int_{\mathbf{R}^2} \nabla \cdot \left[\frac{\nabla u}{|\nabla u|} \right] \psi_{j,k} dx + 2\lambda_{j,k} (\beta_{j,k} - \alpha_{j,k}) = 0 \quad (6)$$

2.2. Our proposed models

Motivated by the previous works[15][16][21], we propose a novel fractional-order p -Laplace TV inpainting model for spatial domain damaged images. The fractional-order p -Laplace TV inpainting model for noiseless images (Model I) is:

$$\min J[u] = \frac{1}{p} \int_{E \cup \Omega} |\nabla^\alpha u|^p dx dy, \alpha \in \mathbf{R}^+, p \in [1, 2] \quad (7)$$

and the fractional-order p -Laplace TV inpainting model for noisy images (Model II) is:

$$\min J_\lambda[u] = \frac{1}{p} \int_{E \cup \Omega} |\nabla^\alpha u|^p dx dy + \frac{\lambda_\Omega}{2} \int_E |u - u_0|^2 dx dy, \alpha \in \mathbf{R}^+, p \in [1, 2] \quad (8)$$

with the Neumann boundary condition $\partial u / \partial n = 0$ on $\partial\Omega$,

$$\text{where } \lambda_\Omega = \lambda \cdot \mathbf{1}_E(x, y) = \begin{cases} \lambda, & (x, y) \in E \\ 0, & \text{otherwise} \end{cases}.$$

In (7) and (8), we use the fractional-order gradient instead of the integral-order gradient. In literature[2], the authors got good results in inpainting non-texture parts, but the integral-order TV inpainting model brings artifacts which can cause bad visual effect. The fractional-order gradient in the PDEs scheme has showed better restoration ability[15][16].

For the images with damaged wavelet coefficients, we present a new fractional-order p -Laplace TV wavelet inpainting model inspired by literature[22]. Likewise, there are two models for both noiseless and noisy images. The fractional-order p -Laplace TV wavelet inpainting model for noiseless images (Model III) is:

$$\min_{\beta_{j,k}: (j,k) \in I} J(u, z) = \frac{1}{p} \int_{\mathbf{R}^2} |\nabla_x^\alpha u(\beta, x)|^p dx, \alpha \in \mathbf{R}^+, p \in [1, 2], \quad (9)$$

where $u(\beta, x)$ has the wavelet transform:

$$u(\beta, x) = \sum_{j,k} \beta_{j,k} \psi_{j,k}(x), \quad \beta = (\beta_{j,k}), j \in \mathbf{Z}, k \in \mathbf{Z}^2,$$

and subjects to the constraint:

$$\beta_{j,k} = \alpha_{j,k}, (j, k) \notin I,$$

where I is the inpainting index region.

The fractional-order p -Laplace TV wavelet inpainting model for noisy images (Model IV) is:

$$\min_{\beta_{j,k}} J_\lambda(u, z) = \frac{1}{p} \int_{\mathbf{R}^2} |\nabla_x^\alpha u(\beta, x)|^p dx + \sum_{(j,k)} \lambda_{j,k} (\beta_{j,k} - \alpha_{j,k})^2, \alpha \in \mathbf{R}^+, p \in [1, 2] \quad (10)$$

and the parameter $\lambda_{j,k}$ is zero if $(j, k) \in I$, the missing index set; otherwise, it equals a positive constant λ to be properly selected. Compared to original work[20], we use the p -Laplace and fractional-order gradient instead of the normal total variation term and the integral gradient.

Because all the models we proposed have the fractional gradient and there is no Euler-Lagrange equation for the fractional calculus, it is necessary to deduce fractional Euler-Lagrange equation.

We use the Model I to deduce the equation. To get the extremum of the energy function, the necessary condition is $\delta J = 0$ according to the variation method.

Let

$$\phi(a) = \frac{1}{p} \int_{E \cup \Omega} |\nabla^\alpha u + a \nabla^\alpha \eta|^p dx dy = \int_{E \cup \Omega} r(|\nabla^\alpha u + a \nabla^\alpha \eta|) dx dy \quad (11)$$

where $r(s) = s^p/p, p \in [1, 2]$ and $\eta(x, y) \in C^\infty(E \cup \Omega)$ is any test function. So

$$\delta J = \frac{\partial}{\partial a} \phi(a) |_{a=0} = \int_{E \cup \Omega} r'(|\nabla^\alpha u + a \nabla^\alpha \eta|) \frac{D_x^\alpha u + a D_x^\alpha \eta}{|\nabla^\alpha u + a \nabla^\alpha \eta|} D_x^\alpha \eta dx dy |_{a=0} + \int_{E \cup \Omega} r'(|\nabla^\alpha u + a \nabla^\alpha \eta|) \frac{D_y^\alpha u + a D_y^\alpha \eta}{|\nabla^\alpha u + a \nabla^\alpha \eta|} D_y^\alpha \eta dx dy |_{a=0} \quad (12)$$

$$= \int_{E \cup \Omega} r'(|\nabla^\alpha u|) \left(\frac{D_x^\alpha u}{|\nabla^\alpha u|} D_x^\alpha \eta + \frac{D_y^\alpha u}{|\nabla^\alpha u|} D_y^\alpha \eta \right) dx dy$$

and $\nabla^\alpha = (D_x^\alpha, D_y^\alpha)$.

Let $D_x^{\alpha*}$ and $D_y^{\alpha*}$ to be the adjoint of D_x^α and D_y^α and the definition is

$$\begin{cases} D_x^{\alpha*} [u(x, y)] = D_x^\alpha [u(-x, y)] \\ D_y^{\alpha*} [u(x, y)] = D_y^\alpha [u(x, -y)] \end{cases}$$

According to the theory of adjoint operator in functional analysis[33], we can get

$$\delta J = \int_{E \cup \Omega} \left[D_x^{\alpha*} \left(r'(|\nabla^\alpha u|) \frac{D_x^\alpha u}{|\nabla^\alpha u|} \right) + D_y^{\alpha*} \left(r'(|\nabla^\alpha u|) \frac{D_y^\alpha u}{|\nabla^\alpha u|} \right) \right] \eta dx dy. \quad (13)$$

For the arbitrariness of η , the Euler-Lagrange equation is

$$D_x^{\alpha*} \left(r'(|\nabla^\alpha u|) \frac{D_x^\alpha u}{|\nabla^\alpha u|} \right) + D_y^{\alpha*} \left(r'(|\nabla^\alpha u|) \frac{D_y^\alpha u}{|\nabla^\alpha u|} \right) = 0. \quad (14)$$

Define the fractional divergence operator $div^\alpha(\cdot)$ as

$$div^\alpha(u) = (-1)^\alpha (D_x^{\alpha*} u + D_y^{\alpha*} u). \quad (15)$$

When $\alpha = 1$, we can easily obtain

$$div(u) = D_x u + D_y u,$$

so it is obvious that the fractional divergence operator is a generalization of integral divergence operator in its general sense. With the definition of fractional divergence operator, we get $r(\cdot)$ (as formerly defined) and (14) into (15) and obtain

$$\overline{(-1)^\alpha} div^\alpha \left(\frac{\nabla^\alpha u}{|\nabla^\alpha u|^{2-p}} \right) = 0. \quad (16)$$

The Euler-Lagrange equations of Model I to Model IV are

Model I:

$$\overline{(-1)^\alpha} div^\alpha \left(\frac{\nabla^\alpha u}{|\nabla^\alpha u|^{2-p}} \right) = 0, \alpha \in \mathbf{R}^+, p \in [1, 2], \quad (17)$$

Model II:

$$\overline{(-1)^\alpha} div^\alpha \left(\frac{\nabla^\alpha u}{|\nabla^\alpha u|^{2-p}} \right) + \lambda_\Omega (u - u_0) = 0, \alpha \in \mathbf{R}^+, p \in [1, 2], \quad (18)$$

$$\lambda_\Omega = \lambda \cdot \mathbf{1}_E(x, y) = \begin{cases} \lambda, (x, y) \in E \\ 0, otherwise \end{cases}$$

Model III:

$$- \int_{\mathbf{R}^2} \overline{(-1)^\alpha} div^\alpha \left(\frac{\nabla^\alpha u}{|\nabla^\alpha u|^{2-p}} \right) \psi_{j,k} dx = 0, \alpha \in \mathbf{R}^+, p \in [1, 2], (j, k) \in I, \quad (19)$$

and Model IV:

$$- \int_{\mathbf{R}^2} \overline{(-1)^\alpha} div^\alpha \left(\frac{\nabla^\alpha u}{|\nabla^\alpha u|^{2-p}} \right) \psi_{j,k} dx + 2\lambda_{j,k} (\beta_{j,k} - \alpha_{j,k}) = 0, \alpha \in \mathbf{R}^+, p \in [1, 2], \quad (20)$$

$$\lambda_{j,k} = \lambda \cdot \mathbf{1}_I(j, k) = \begin{cases} 0, (j, k) \in I \\ \lambda, otherwise \end{cases}$$

Our method can be seen as a generalized image inpainting framework with both integral- and fractional-order and it is easy to extend to other image inpainting with PDEs methods, even the denoising models, such as CDD[5], BSCB[1], Mumford-Shah-Euler model[4], TV-Stokes equation[23], et al. The reason we give the fractional-order TV image inpainting model here is that the TV model which is both used in inpainting and denoising is representative and the discrete algorithm is relatively simple.

In this paper, an adaptive factor p is proposed based on the local geometry and gradient features of images. The p is defined as followed:

$$p = 1 + \frac{curv^\alpha}{curv^\alpha + |\nabla^\alpha u|}$$

where $curv^\alpha$ is defined below, as the fractional curvature formula for level lines of u .

3. Numerical algorithm

There are many numerical algorithms[24][25][26] available to get the minimizations of the proposed models. The computation used for current work has been mainly based on the gradient descent method, which is not the most efficient. We primarily aim at the discretization of the fractional framework and exploring the inpainting feasibility and qualities of the models rather than their numerical algorithms.

We get the gradient flow by introducing an artificial time variable and solving the equations followed to steady states for Model I to IV respectively,

$$u_t = \overline{(-1)^\alpha} \operatorname{div}^\alpha \left(\frac{\nabla^\alpha u}{|\nabla^\alpha u|^{2-p}} \right), \tag{21}$$

$$u_t = \overline{(-1)^\alpha} \operatorname{div}^\alpha \left(\frac{\nabla^\alpha u}{|\nabla^\alpha u|^{2-p}} \right) + \lambda_\Omega (u - u_0), \tag{22}$$

$$(\beta_{j,k})_t = - \int_{\mathbf{R}^2} \overline{(-1)^\alpha} \operatorname{div}^\alpha \left(\frac{\nabla^\alpha u}{|\nabla^\alpha u|^{2-p}} \right) \psi_{j,k} dx, \tag{23}$$

and

$$(\beta_{j,k})_t = - \int_{\mathbf{R}^2} \overline{(-1)^\alpha} \operatorname{div}^\alpha \left(\frac{\nabla^\alpha u}{|\nabla^\alpha u|^{2-p}} \right) \psi_{j,k} dx + 2\lambda_{j,k}(\beta_{j,k} - \alpha_{j,k}). \tag{24}$$

The equations mentioned above are deduced from the Euler-Lagrange Equations (17) to (20) and the parameters here are same.

Firstly, we describe the discretization of the fractional gradient operator ∇^α with Grünwald-Letnikov definition[19] in fractional calculus as the mask we proposed in literature[27]. We also explained the reason why we chose the masks defined by Grünwald-Letnikov definition in it.

α -order Grünwald-Letnikov definition based fractional differential can be expressed by

$$D_{G-L}^\alpha s(x) = \left. \frac{d^\alpha}{[d(x-a)]^\alpha} s(x) \right|_{G-L} = \lim_{N \rightarrow \infty} \frac{(x-a)^{-\alpha}}{\Gamma(-\alpha)} \sum_{k=0}^{N-1} \frac{\Gamma(k-\alpha)}{\Gamma(k+1)} \times s(x - k(\frac{x-a}{N})) \tag{25}$$

where the duration of signal $s(x)$ is $[a, x]$, α is any real number, and $s(x - k((x-a)/N))$ is the discrete sampling.

When N is big enough, one can get rid of the limits symbol and rewrite (25) as

$$\left. \frac{d^\alpha}{dx^\alpha} s(x) \right|_{G-L} \cong \frac{x^{-\alpha} N^\alpha}{\Gamma(-\alpha)} \sum_{k=0}^{N-1} \frac{\Gamma(k-\alpha)}{\Gamma(k-1)} s(x + \frac{\alpha x}{2N} - \frac{kx}{N}). \tag{26}$$

To get the value of $s(x + \alpha x/2N - kx/N)$, we use Lagrange 3-point interpolation with $s(x + x/N - kx/N)$, $s(x - kx/N)$, and $s(x - x/N - kx/N)$. Then we get

$$\frac{d^\alpha}{dx^\alpha} s(x) \cong \frac{x^{-\alpha} N^\alpha}{\Gamma(-\alpha)} \sum_{k=0}^{N-1} \frac{\Gamma(k-\alpha)}{\Gamma(k+1)} \times \left[s_k + \frac{\alpha}{4}(s_{k-1} - s_{k+1}) + \frac{\alpha^2}{8}(s_{k-1} - 2s_k + s_{k+1}) \right]. \tag{27}$$

When $k = n \leq N-1$, from (26), the anterior $n+2$ approximate backward difference of fractional partial differential respectively on negative x-and y-axis, are expressed as

$$\frac{\partial^\alpha s(x,y)}{\partial x^\alpha} \cong a_1 s(x+1, y) + a_2 s(x, y) + a_3 s(x-k, y) + a_4 s(x-n+1, y) + a_5 s(x-n, y), \tag{28}$$

and

$$\frac{\partial^\alpha s(x,y)}{\partial y^\alpha} \cong a_1 s(x, y+1) + a_2 s(x, y) + a_3 s(x, y-k) + a_4 s(x, y-n+1) + a_5 s(x, y-n), \tag{29}$$

where

$$\begin{aligned} a_1 &= \frac{\alpha}{4} + \frac{\alpha^2}{8}, \\ a_2 &= 1 - \frac{\alpha^2}{2} - \frac{\alpha^3}{8}, \\ a_3 &= \frac{1}{\Gamma(-\alpha)} \sum_{k=1}^{n-2} \left[\frac{\Gamma(k-\alpha+1)}{(k+1)!} \left(\frac{\alpha}{4} + \frac{\alpha^2}{8} \right) + \frac{\Gamma(k-\alpha)}{k!} \left(1 - \frac{\alpha^2}{4} \right) + \frac{\Gamma(k-\alpha-1)}{(k-1)!} \left(-\frac{\alpha}{4} + \frac{\alpha^2}{8} \right) \right], \\ a_4 &= \frac{\Gamma(n-\alpha-1)}{(n-1)! \Gamma(-\alpha)} \left(1 - \frac{\alpha^2}{4} \right) + \frac{\Gamma(n-\alpha-2)}{(n-2)! \Gamma(-\alpha)} \left(-\frac{\alpha}{4} + \frac{\alpha^2}{8} \right), \\ a_5 &= \frac{\Gamma(n-\alpha-1)}{(n-1)! \Gamma(-\alpha)} \left(-\frac{\alpha}{4} + \frac{\alpha^2}{8} \right). \end{aligned} \tag{30}$$

For simplicity, we only use four directions fractional-order masks for calculation, including positive x- and y-coordinate, negative x- and y-axis. Let D_{x+}^α , D_{x-}^α , D_{y+}^α and D_{y-}^α denote the four directions calculation, see Fig.1. It is easy to say that bigger the mask size is, a higher degree of accuracy we will get, but the computational time will be consuming. Considering the analysis in literature[27], we fix the size of mask to 5.

The coefficients of masks in Fig.1 are:

$$\left\{ \begin{aligned} C_{s_{-1}} &= \frac{\alpha}{4} + \frac{\alpha^2}{8}, \\ C_{s_0} &= 1 - \frac{\alpha^2}{2} - \frac{\alpha^3}{8}, \\ C_{s_1} &= -\frac{5\alpha}{4} + \frac{5\alpha^2}{16} + \frac{\alpha^4}{16}, \\ &\vdots \\ C_{s_k} &= \frac{1}{\Gamma(-\alpha)} \left[\frac{\Gamma(k-\alpha+1)}{(k+1)!} \left(\frac{\alpha}{4} + \frac{\alpha^2}{8} \right) + \frac{\Gamma(k-\alpha)}{k!} \left(1 - \frac{\alpha^2}{4} \right) + \frac{\Gamma(k-\alpha-1)}{(k-1)!} \left(-\frac{\alpha}{4} + \frac{\alpha^2}{8} \right) \right], \\ &\vdots \\ C_{s_{n-2}} &= \frac{1}{\Gamma(-\alpha)} \left[\frac{\Gamma(n-\alpha-1)}{(n-1)!} \left(\frac{\alpha}{4} + \frac{\alpha^2}{8} \right) + \frac{\Gamma(n-\alpha-2)}{(n-2)!} \left(1 - \frac{\alpha^2}{4} \right) + \frac{\Gamma(n-\alpha-3)}{(n-3)!} \left(-\frac{\alpha}{4} + \frac{\alpha^2}{8} \right) \right], \\ C_{s_{n-1}} &= \frac{\Gamma(n-\alpha-1)}{(n-1)! \Gamma(-\alpha)} \left(1 - \frac{\alpha^2}{4} \right) + \frac{\Gamma(n-\alpha-2)}{(n-2)! \Gamma(-\alpha)} \left(-\frac{\alpha}{4} + \frac{\alpha^2}{8} \right), \\ C_{s_n} &= \frac{\Gamma(n-\alpha-1)}{(n-1)! \Gamma(-\alpha)} \left(-\frac{\alpha}{4} + \frac{\alpha^2}{8} \right). \end{aligned} \right. \tag{31}$$

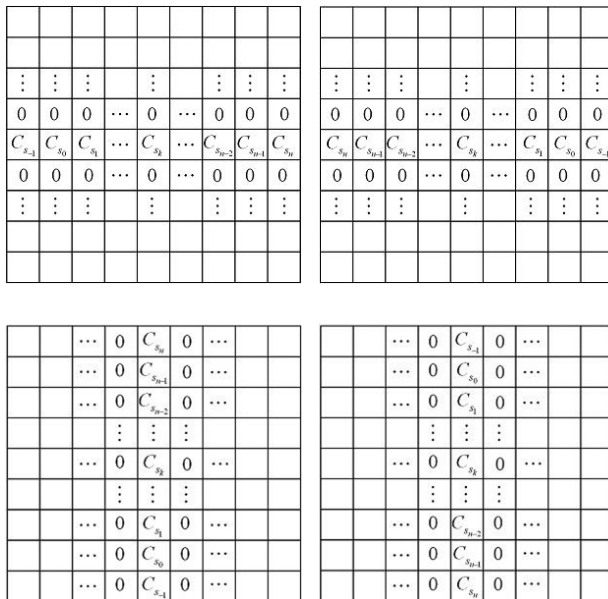


Figure 1 Masks of four directions. (a) D_{x+}^α ; (b) D_{x-}^α ; (c) D_{y+}^α ; (d) D_{y-}^α

So we get the discrete representation of the most important item:

$$\begin{aligned}
 \text{curl}^\alpha &= \text{div}^\alpha \left(\frac{\nabla^\alpha u}{|\nabla^\alpha u|^{2-p}} \right) = \\
 D_{x-}^\alpha &\left(\frac{D_{x+}^\alpha u}{(|D_{x+}^\alpha u|^2 + |D_{y+}^\alpha u|^2 + \varepsilon)^{\frac{2-p}{2}}} \right) \\
 + D_{y-}^\alpha &\left(\frac{D_{y+}^\alpha u}{(|D_{x+}^\alpha u|^2 + |D_{y+}^\alpha u|^2 + \varepsilon)^{\frac{2-p}{2}}} \right)
 \end{aligned} \tag{32}$$

where ε is a small positive number to prevent dividing by zero.

4. Simulations

In our simulations, we use the Peak Signal to Noise Ratio (PSNR) to quantify the performance of inpainting algorithms:

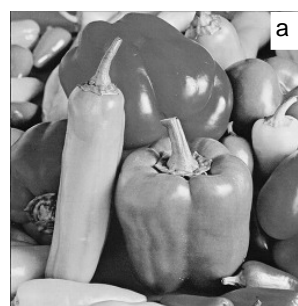
$$PSNR = 10 \times \log_{10} \left(\frac{255^2}{\|u - u_0\|_2^2} \right).$$

Bigger the value of PSNR is, better the performance is. The test 256×256 grayscale images include peppers, lena, house and barbara.

The proper selection of the fractional order α depends on the image to inpaint. We have test the order from 0.1 to 3.0 with step 0.1 on every testing images and we find that $\alpha \approx 1.8$ can get the best results on Model I, $\alpha \approx 1.6$ on

Model II, $\alpha \approx 1.2$ on Model III and IV. So in this paper, the order selection is based on the simulation experience and the theoretical analysis and derivation will be our following works.

4.1. Model I



b
 Inpainting is an image interpolation problem, often referring to interpolations over large-scale missing domains. In this paper, guided by the

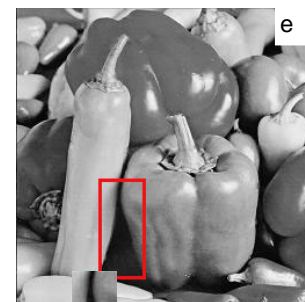
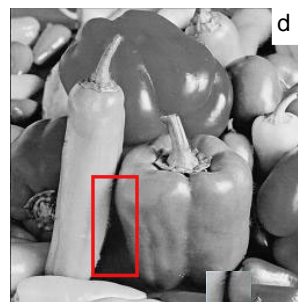
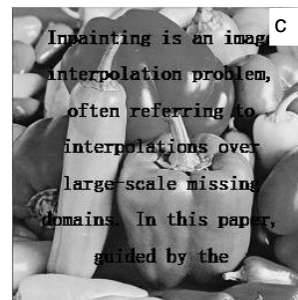


Figure 2 Inpainting results comparison of TV and Model I on peppers. (a) Original image; (b) Mask; (c) Damaged image (PSNR=15.8213); (d) TV inpainting (PSNR=36.1233); (e) Model I (PSNR=38.0236, $\alpha = 1.8$); (f) Zoom of red block of (d); (g) Zoom of red block of (e);

Fig.2 shows the result of text removal on peppers compared with original integral-order TV inpainting using Model I. All the parameters are set as proposed [2]. For the inpainting performance, when we choose the proper parameter, we got a better PSNR than integral-order TV model.

For the visual effect, focusing on the Fig. (2f) and Fig. (2g), we can see that at the edge between two peppers, integral-order TV can not connect the broken edge perfectly, but our method got a satisfactory result and the edge was reconnected as expected. The reason is that the original TV inpainting model is second-order and when $\alpha = 1.8$, the Model I is close to third-order.

Table 1 Results of other three test images(PSNR)

	Damaged image	TV inpainting	Our method
Lena	15.8834	34.4429	36.2158
House	16.4599	35.8064	36.7274
Barbara	14.9861	32.7660	32.7759

The inpainting results with the same damaged mask, Fig.4.1, of other three images are displayed in the Tab.1(α remains 1.8). While inpainting lena and house, the PSNR values of Model I are bigger than original TV inpainting model, but there is no obvious difference while dealing with barbara. The reason is that barbara is full of texture details and the PDE methods have intrinsic flaw to handle this, but we can combine some other ideas to recover it, such as nonlocal method[28].

4.2. Model II

Fig.3 shows the result of scratch removal on noisy lena compared with original integral-order TV inpainting using Model II. We can see that the scratches on the images are almost repaired by both integral- and fractional-order TV inpainting model, but when zooming out the face of lena, there are still traces on the right eye and left eyebrow in Fig. (3e), and stair effect appeared [29][30][31] on lena's cheek. From Fig. (3f), there is no noticeable inpainting consequence and no stair effect on lena's face. The noise removal ability of fractional-order PDE model is analyzed in [16][15][32].

4.3. Model III

We use Daubechies 7-9 biorthogonal wavelets with symmetric extensions, which is used in standard JPEG2000 for lossy compression. We use the WaveLab[34] to implement the forward and the backward biorthogonal wavelet transforms. The size of coarsest subband is 32×32 . The parameters of original TV wavelet inpainting model are set as proposed[20]. We applied Model III to lena with 10% wavelet coefficients randomly loss, see Fig.4.

Because the loss of coefficients is on all four subband, including LL, HH, LH and HL, there are not only block loss, but also oscillations. From Fig.4, we can see both original TV wavelet inpainting model and Model III eliminate the small oscillations, but in Fig. (4c), blocks near

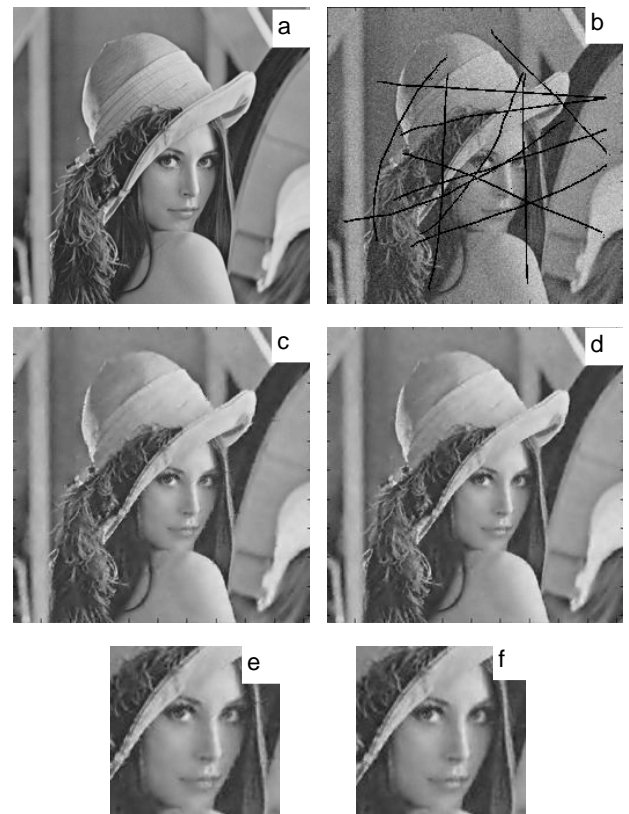


Figure 3 Inpainting results comparison of TV and Model II on lena. (a) Original image; (b) Damaged image with $\sigma = 20\%$ Gaussian Noise (PSNR=17.1900); (c) TV inpainting (PSNR=24.2052); (d) Model II (PSNR=25.1206, $\alpha = 1.6$); (e) Zoom of lena's face of (c); (f) Zoom of lena's face of (d);

the lena's hair are not removed completely. Although in Fig. (4d), there are blocks at the same position, the edges are obvious and the PSNR is bigger. When the loss of the coefficients gets larger, the difference of inpainting performance between integral- and fractional-order model is fainter.

4.4. Model IV

In this part, we compared the original TV wavelet with Model IV while dealing noisy image. In Fig.5, the noisy level is $\sigma = 20\%$, and loss of coefficients is 50%. From Fig. (5b), we can find that the most details are lost, and it is hard to get any useful information without the deep impression of famous lena. After processed by both model, the results are in Fig. (5c) and Fig. (5d). The main content is repaired by inpainting, but the performances of two models are still different. The larger blocks caused by coefficients loss can not be removed by both methods, but the size of them is smaller in Model IV than original TV



Figure 4 Inpainting results comparison of TV wavelet and Model III on lena. (a) Original image; (b) Received image with 10% wavelet coefficients loss (PSNR=17.1900); (c) TV inpainting (PSNR=24.2052); (d) Model III (PSNR=25.1206, $\alpha = 1.4$)

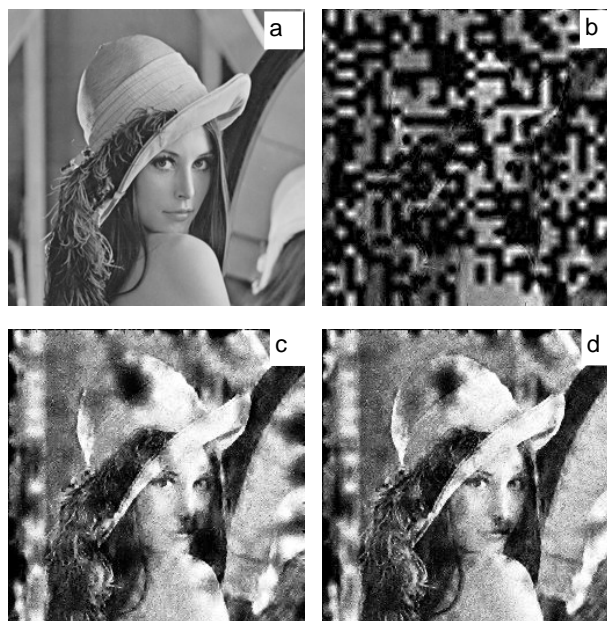


Figure 5 Inpainting results comparison of TV wavelet and Model IV on lena. (a) Original image; (b) Received image with 50% wavelet coefficients loss and $\sigma = 20\%$ Gaussian Noise(PSNR=7.3664); (c) TV inpainting (PSNR=14.0809); (d) Model IV (PSNR=15.0446, $\alpha = 1.4$)

wavelet inpainting model and the PSNR is larger too. To give a complete demonstration about the comparison of different, we draw the curves for PSNR improvements v.s. the percentage of lost coefficients for $\sigma = 20\%$ Gaussian noisy image in Fig.6. As we can see, Model IV outperforms original TV wavelet inpainting model in almost every coefficients loss level, except 0.9.

5. Conclusion

In this paper we propose four image models based on fractional total variation. The models can both deal with space and wavelet domain damages for images with or without noise. In simulation part, we show that our models are better than original inpainting models based on integral-order total variation in both visual effect and PSNR. The relationship between fractional order and the inpainting performance will be our following work, and an adaptive fractional model will be very useful in practical applications.

References

[1] M. Bertalmio, G. Sapiro, V. Caselles and C. Ballester, *Proc. SIGGRAPH*, **2000**, 417 (2000).
 [2] T. F. Chan and J. Shen, *SIAM J. Appl. Math.* **62**, 1019 (2001).
 [3] L. Rudin, S. Osher and E. Fatemi, *Phys. D* **60**, 259 (1992).

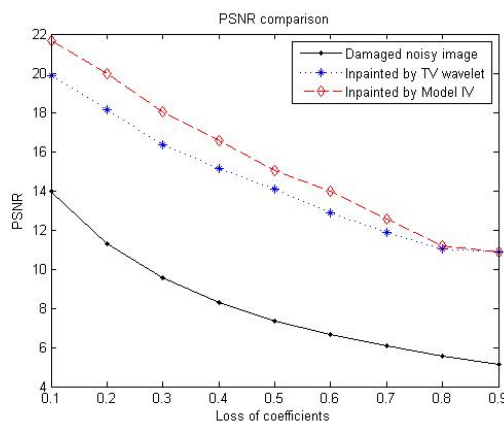


Figure 6 The performance comparisons of original TV wavelet inpainting model and Model IV with different level of damages for noisy image. It shows that both models can improve the image quality significantly, but Model IV is more effective.

- [4] D. Mumford and J. Shah, *Comm. Pure Applied Math.* **XLII**, 577 (1989).
- [5] T. F. Chan and J. Shen, *J. Visual Comm. Image Rep.* **12**, 436 (2001).
- [6] M. Bertalmio, L. Vese, G. Sapiro and S. Osher, *IEEE Trans. Image Process.* **12**, 882 (2003).
- [7] A. A. Efros and T. K. Leung, *Proc. ICCV1999*, 1033 (1999).
- [8] S. Masnou, *IEEE Trans. Image Process.* **11**, 68 (2002).
- [9] M. Bertalmio, *IEEE Trans. Image Process.* **15**, 1934 (2006).
- [10] E. Cuesta and J. F. Codes, *Proc. ICVIP*, **2003**, 438 (2003).
- [11] R. Duits, M. Felsberg, L. Florack and B. Platel, *LNCS* **2695**, 494 (2003).
- [12] S. Didas, B. Burgeth, A. Imiya and J. Weickert, *LNCS* **3459**, 13 (2005).
- [13] B. Mathieu, P. Melchior, A. Oustaloup and Ch. Ceyral, *Signal Process.* **83**, 2421 (2003).
- [14] Y.-F. Pu, W.-X. Wang, J.-L. Zhou, Y.-Y. Wang and H.-D. Jia, *Sci. China Ser. F: Inform. Sci.* **51**, 1319 (2008).
- [15] P. Guidotti and J. V. Lambers, *J. Math. Imaging Vis.* **33**, 25 (2009).
- [16] J. Bai and X. Feng, *IEEE Trans. Image Process.* **16**, 2492 (2007).
- [17] Y. Zhang, Y.-F. Pu, J.-R. Hu, Y. Liu and J.-L. Zhou, *J. X-ray Sci. Technol.* **19**, 373 (2011).
- [18] Y. Zhang, Y.-F. Pu, J.-R. Hu, Y. Liu, Q.-L. Chen and J.-L. Zhou, *Comput. Math. Method M.* **2011**, 173748 (2011).
- [19] K. B. Oldham and J. Spanier, *The Fractional Calculus*, (Academic Press, New York, 1974).
- [20] T. F. Chan, J. Shen and H.-M. Zhou, *J. Math. Imaging Vis.* **25**, 107 (2006).
- [21] A. Kristaly, H. Lisei and C. Varga, *Nonlinear Analysis-Theory Methods & Applications* **5**, 1375 (2008).
- [22] H. Zhang, Q. Peng and Y. Wu, *Acta Auto. Sinica* **25**, 107 (2006).
- [23] X. C. Tai, S. Osher and R. Holm, *Proc. Int. Conf. PDE-Based Image Process. Related Inverse Problem* **2007**, 3 (2007).
- [24] S. Osher, M. Burger, D. Goldarb, J. Xu and W. Yin, *Multiscale Model. Simul.* **4**, 460 (2005).
- [25] A. Chambolle, *J. Math. Imaging Vis.* **20**, 89 (2004).
- [26] X. Zhang, M. Burger and S. Osher, *J. Sci. Comput.* **46**, 20 (2010).
- [27] Y.-F. Pu, J.-L. Zhou and X. Yuan, *IEEE Trans. on Image Process.* **19**, 491 (2010).
- [28] G. Gilboa and S. Osher, *Multiscale Model. Simul.* **7**, 1005 (2008).
- [29] T. F. Chan, A. Marquina and P. Mulet, *SIAM J. Sci. Comput.* **22**, 503 (2000).
- [30] Y. L. You and M. Kaveh, *IEEE Trans. Image Process.* **9**, 1723 (2000).
- [31] M. Lysaker, A. Lundervold and X. C. Tai, *IEEE Trans. Image Process.* **12**, 1579 (2003).
- [32] Y.-F. Pu, Yi Zhang and J.-L. Zhou, Fractional partial differential equation: texture image restoration based on fractional total variation and fractional extreme point, *Submitted to IEEE Trans. on Image Process.*
- [33] A. N. Kolmogorov and S. V. Fomin, *Elements of The Theory of Functions And Functional Analysis*, (Dover Publications, Mineola, 1999).
- [34] <http://www-stat.stanford.edu/~wavelab/>



Yi Zhang received the B.S. and M.S. degrees from College of Computer Science, Sichuan University, China, and now he is a Ph.D. Student at Sichuan University. He has published several papers of which are indexed by SCI, EI, or ISTP. His interested research is image processing with partial differential equation.



Yi-Fei Pu received the B.S., M.S., and Ph.D. Degrees from the School of Electronics and Telecommunication, Sichuan University, China, and continued his postdoctoral study respectively at the University of Electronic Science and Technology of China, Nancy University I, and the University of Paris 12, France. He is an Associate Professor with the School of Computer Science and Technology, Sichuan University. He studies the application of fractional calculus in the latest signal analysis and processing.



Jin-Rong Hu received the B.S. and M.S. degrees from College of Computer Science, Sichuan Normal University, China, and now she is a Ph.D. Student at Sichuan University. Her interested research is image processing with partial differential equation.



Ji-Liu Zhou is a Professor with College of Computer Science, Sichuan University, China. He is the academic leader of Sichuan Province and has held 17 state or provincial scientific projects, including key projects supported by National Science Foundation. His research is mainly in the field of image processing, artificial intelligence, fractional calculus application in the latest signal and image processing, and so on. He has published more than 100 papers, of which more than 80 papers are indexed by SCI, EI, or ISTP.